

Submicromolar quantification of pyocyanin in complex biological fluids using pad-printed carbon electrodes

Richard Burkitt and Duncan Sharp*

Centre for Biomedical Science Research, School of Clinical and Applied Sciences, Leeds Beckett University, Leeds, LS1 3HE, United Kingdom

*Corresponding author: T: +44(0)113 812 9398 E: d.sharp@leedsbeckett.ac.uk

Abstract

Pyocyanin, a toxin produced by *Pseudomonas aeruginosa*, offers potential as a biomarker for the indirect detection of this bacterium of major importance for infections in burns, woundcare and cystic fibrosis.

Pad-printed carbon electrodes are herein explored using square wave voltammetry to detect pyocyanin in a range of buffered and biological media. Third-order polynomial baseline fitting was explored to enhance the analytical sensitivity and extend the linear range to submicromolar concentrations. These modelling baselines showed excellent correlation with the experimental data, confirmed by high Interclass Correlation Coefficients of 0.995 – 0.998, and enabled the quantification of pyocyanin – with linearity extended down to 0.18 μ M in Human Serum and 0.336 μ M in both Britton-Robinson buffer and Simulated Wound Fluid, and derived Limits of Detection of 0.17, 0.15 and 0.09 μ M, respectively, in this proof-of-concept study.

Therefore, the use of very simple, cost-effective printed carbon materials enabled the detection of clinically relevant concentrations of this important biomarker through a new baseline fitting model and offers a novel approach for point-of-care diagnostics where *Pseudomonas aeruginosa* infections are critical.

Keywords: Pyocyanin, Human Serum, Wounds, Voltammetry, *Pseudomonas aeruginosa*.

1. Introduction

The ability to rapidly quantify biomarkers through point-of-care testing (PoCT) confers a huge advantage for the rapid diagnosis and controlled management of many diseases and conditions. New analytical methodologies and platforms are essential to drive these technologies forward thereby enabling PoCT to cover a wider range of diagnoses. An area where this is apparent is within woundcare and burns management; a recent eDEPLHI study found that clinician's top research priorities included the development of wound diagnostics and the management of wound infections [1]. Research towards PoCT to enhance woundcare have been targeted through standard *in-vitro* diagnostic approaches, but also the emerging concept of smart-bandages, capable of providing diagnostic information and detecting wound infection without the need for wound redressing using many electrochemical approaches [2-7].

One biomarker we have previously suggested is pyocyanin – a toxin produced by *Pseudomonas aeruginosa* infections – of particular importance in woundcare, burns and cystic fibrosis. The ability to reliably and sensitively measure pyocyanin has been approached through electrochemical means, such as the use of gold-electrode arrays to map pyocyanin production through agar-diffusion model [8], commercial carbon strip electrodes [9,10], and carbon fibre and glassy carbon [11]. Previous research has shown that such technologies have been capable of producing small calculated Limits of Detection, but often being unable to quantify pyocyanin below 1 μ M [9,11]. The ability to develop sensitive analytical technologies to quantify pyocyanin, enabling rapid diagnosis or more specific management, would be of benefit to patients and healthcare providers. Physiologically and diagnostically relevant concentrations have yet to be fully determined; concentrations as high as 130 μ M have been identified in the sputa of cystic fibrosis patients [12], but more generally (and in wounds), concentrations <10 μ M are more commonly found [13]. In terms of the physiological relevance of pyocyanin, a dose dependent formation of hydrogen peroxide in endothelial cells for 1 – 50 μ M pyocyanin, concentrations of 5-10 μ M have been found to arrest cell growth, and 25 μ M to induce apoptosis (14, 15).

The research detailed herein explores the proof-of-concept use of a non-modified printed carbon electrode using square wave voltammetry through simple peak-current analysis, and analysis following third-order polynomial baseline fitting. The use of baseline fitting or subtraction models have attracted some interest in electroanalytical chemistry –with

asymmetric least squares and polynomial baselines shown to enhance detection, produce better calibration plots and enable lower Limits of Detection [16-20]. The research detailed here explores the potential use of a third-order polynomial baseline fitting to enhance pyocyanin detection (Limits of Detection, Quantification and Linearity) in buffered and authentic biological media.

2. Material and methods

2.1 Materials and Chemicals

All chemicals used were of reagent grade and used without further purification. Britton Robinson buffer (BR) was prepared from 40mM of acetic, boric and phosphoric acids and adjusted to pH 7.0 prior to use. Simulated Wound Fluid (SWF) was prepared from 50% Equine Serum (Sigma Aldrich H1270) and 50% maximum recovery diluent (4.25 g/L NaCl (BDH) and 0.5g/L MC-19 Beef Extract (Lab M)). Human Serum (H6914) and pyocyanin (P0046) (from *Pseudomonas aeruginosa* ($\geq 98\%$)), were purchased from Sigma-Aldrich, and kept frozen (-20°C) until use.

2.2 Preparation of Pad Printed Electrodes

The pad printing process of electrodes was performed as previously described [4]. Carbon Graphite Ink (Gwent Group-C2000802P2) was thinned with isophorone to produce an ink of consistent viscosity. After printing two carbon layers ($\sim 5\mu\text{m}$ each), isophorone was evaporated through 18 hours in a fume hood and then heated at 90°C for 30min. Dielectric paste (Gwent Group) was diluted with Diluent (Gwent Group-S70204D5) and printed followed by the same evaporation and thermal treatment step, defining a working electrode of an exposed area of $\sim 5.6\text{mm}^2$. Electrical connection was made through conductive adhesive copper tape (Farnell, UK).

2.3 Electrochemical experiments

Electrochemical detection of pyocyanin was carried out in a three-electrode set-up using printed carbon working and counter electrodes, and a 3M NaCl Ag/AgCl reference electrode (BASi). All electrochemical measurements were performed using Square Wave Voltammetry (SqWV) [$a=100\text{mV}$, $f=2.2\text{Hz}$.] in 3ml of electrolyte, using a $\mu\text{AutolabIII}$ (Eco Chemie) potentiostat and analysed through NOVA 1.10 software, at room temperature (20°C). Prior to

use, each electrode was electrochemically cleaned with SqWV in the corresponding electrolyte, for five scans -0.45 - +0.1V prior to addition of pyocyanin. The anodic limit was set ($E < 0.1V$) to avoid electropolymerisation of pyocyanin [11].

2.4 Third-order polynomial baseline fitting

Third order polynomial baselines were applied in Nova v1.10 by fitting to acquired data points typically $E =$ (a)-0.4, (b)-0.35, (c)-0.05 and (d) 0V in BRB, either side of the peak, with a 40mV cathodic shift for more alkaline pH. Such an approach was used to create a residual plot, of which the peak oxidation currents could be analysed and interpreted. At very high concentrations peak broadening required cathodic shift of data points (a) and (b) and anodic shift of data points (c) and (d) to linear sections flanking the peak.

2.5 Limits of Detection and Quantification

The Limits of Detection (LoD) and Quantification (LoQ) were determined as $3\sigma/\text{Sensitivity}$ and $10\sigma/\text{sensitivity}$, respectively, where σ is the standard deviation of blank measures ($n=15$), and sensitivity derived as: $\mu A \mu\text{Mole}^{-1} L^{-1}$. These could only be quantified for baseline fitted data due to the absence of anodic peaks observed at zero (and low concentrations) resulting in a standard deviation of zero for unfitted data.

2.6 Statistical analysis

Interclass correlation coefficients were calculated using IBM SPSSv21, with an 'absolute fitting' model, to assess correlation and the quantitative agreement between the baseline fitted model (third-order polynomial) and experimental data.

3. Results and Discussion

The simple carbon electrodes were found capable of detecting pyocyanin ($E_{pa} \sim -0.2V$: pH 7.0), but offered reduced sensitivity at lower concentrations due to the shape of the underlying voltammogram (Figure 1A-C) whereby the basal/graphitic carbon baseline is non-linear across the potential range preventing the reliable peak current integration. The use of a third-order polynomial baseline fitting was explored to correct for the underlying shape prior to peak current integration to assess whether this method of data analysis may yield more sensitive quantification. This was first assessed in pyocyanin-free media to assess the correlation between the unfitted (raw) data and the fitted polynomial baseline corrected data. The analysis

of the full data set ($n=278$ data points / SqWV steps), shows a good agreement through the Interclass Correlation Coefficient (ICC), ranging from 0.986-0.993 for BR buffer, 0.992 for SWF, and 0.994 for HS. However, it is clear from all voltammograms shown in Figure 1, that there is an initial artefactual result at the starting (cathodic) potentials, therefore with the first two data points omitted the agreement for the working range for the SqWV (hereby defined as -0.446 to 0.1V) produced very strong correlations: BR buffer: ICC 0.995-0.997, and SWF and HS both ICC 0.998, indicating the potential applicability of this fitting mode.

The overlaid voltammograms in Figure 1 detail pyocyanin-free and $5\mu\text{M}$ pyocyanin in each media (*lines 1 & 2*), the resulting residual plots (*lines 3 & 4*) pertaining the difference between the unfitted (raw) and aforementioned fitting model (*dashed fitting lines*). The residual plots give rise to clearly defined oxidation peaks, as shown in Figure 1 (A-C) for all three media tested. Importantly, these voltammograms from biological media show no apparent interference from other electroactive species. As expected, there are differences in the peak heights, which may be attributed to the inherent differences in electrolyte properties, potential fouling from biological components, and pH of the media.

Detailed calibration in the three selected media, Figure 2A-C, show the carbon electrodes are capable of producing a clear pyocyanin oxidation peak in each media. The repeated scans performed in establishing the calibration plots give rise to minor deviations in E_{pa} , as detailed in Figure 2D. For the more complex biological media the overall trend remains as a shift towards more cathodic E_{pa} values – which may be attributed to the weaker buffering capacities (potentially exacerbated by the smaller working volumes used in these experiments), or the presence of biological components which may be effecting the electrode surface (e.g. adsorption of proteins and fats).

As shown for all media studied in Figure 3(A&B), a non-linear response is observed across the full range (0-100 μM) of pyocyanin concentrations studied for both the unfitted experimental data (Figure 3A) and baseline fitted data (Figure 3B). This matches the findings of previous research into carbon fibre and glassy carbon electrodes, where we have previously observed this non-linearity for carbon surfaces with higher edge-plane sites (i.e. anodised, but not plain, carbon fibre), and for glassy carbon electrodes. However, the differences between the unfitted and baseline fitted data are highlighted through the lower concentration (0-10 μM) calibration

plots shown for Human Serum (Figure 3C), where the different in axis-intercept and the linear range are clearly illustrated. For all three media tested, Table 1 highlights the basic analytical performance which were achieved throughout this initial testing in the different media.

It is clear that the interpretation of unfitted data provides the quantification of pyocyanin, but due to the background voltammogram shape at the integration potentials, could not quantify pyocyanin below $\sim 1\text{-}2.5\mu\text{M}$. However, as shown in Figure 3C, following the baseline fitting, the lower linear range extends to much lower concentrations of pyocyanin, reflected in the linear ranges that have been quantified for the three electrodes, shown in Table 1, down to $0.183\text{-}0.336\mu\text{M}$ across the three media tested. Not only does the baseline fitted data provide an enhanced linear range, but there is also a small increase in sensitivity ($\mu\text{A}/\mu\text{M}$) observed in each of the three media (BRB +4.0%, SWF +9.7%, HS +9.3%)

Due to the clinical importance of measuring pyocyanin at low concentrations, the Limit of Detection was derived for the measurements performed, as shown in Table 1 for the baseline fitted data. The calculated Limit of Detection for the three electrolytes are similar; 0.150 , 0.087 and $0.169\mu\text{M}$, for BR, SWF and HS respectively, and are in line with those reported in the literature using a range of electrode materials: $0.030\mu\text{M}$ for carbon fibre in buffer [11], $0.6\mu\text{M}$ for gold working electrode in buffer [20], and $0.160\mu\text{M}$ for carbon electrode in heparinised blood [9].

An advantage of using a baseline fitting formula rather than an experimental blank, is that once a sufficient evidence base has been generated and electrode reproducibility enhanced, the baseline equation can be applied in situations whereby a starting blank cannot be performed – and this proof-of-concept study has shown this enables the linear range to extend below $1\mu\text{M}$ for all electrolyte/ media tested.

4. Conclusions

The use of a third-order polynomial baseline fitting model facilitated the submicromolar detection of pyocyanin by simple printed carbon electrodes including in biological media. Given the cost effectiveness and simplicity of the sensing materials required – the advances highlighted within may provide a simple approach to enhancing the sensitivity of voltammetric analysis and a potentially fieldable technology for a novel diagnostic tool.

Figure Legends:

Figure 1. Square Wave Voltammograms for pad-printed carbon electrodes for in 5 μ M pyocyanin[1], pyocyanin free media [2], third-order polynomial baseline fitting lines [*dashed lines*], and residual plots for 5 μ M pyocyanin[3], pyocyanin free media [4]. A. Britton-Robinson buffer (pH 7.0), B. Simulated Wound Fluid (pH 7.3), C. Human Serum (pH 8.35).

Figure 2. Residual plots from third-order baseline fitted square wave voltammograms for the calibration of pyocyanin (0,0.183, 0.334, 0.667, 1, 1.5, 2, 3, 4, 5, 10 μ M). For air saturated: A. Britton-Robinson Buffer (pH 7.0), B. Simulated Wound Fluid (pH 7.3) and C. Human Serum (pH 8.35). D. *Epa* for increasing pyocyanin concentration (0-100 μ M) for the three electrolytes studied (raw and baseline-fitted data).

Figure 3: Pyocyanin calibration plots for unfitted (A) and third-order polynomial baseline fitted data (B), for the full range of pyocyanin concentrations studied (0-100 μ M); Britton-Robinson Buffer pH 7.0 (n=3) shown as mean \pm SD, SWF and HS performed in singlicate. C. Comparison of 0-10 μ M Pyocyanin calibration plots in Human Serum for raw [HS] and baseline fitted data [HS*].

Tables:

Table 1. Analytical performance of the printed carbon electrodes in Britton-Robinson buffer, Simulated Wound Fluid, and Human Serum.

	Britton-Robinson (pH7)		Simulated Wound Fluid		Human Serum	
	Raw	P ³ BF	Raw	P ³ BF	Raw	P ³ BF
Linear range (μ M)	1.0 - 10	0.336 - 10	1.5 - 20	0.336 - 20	2.5 - 20	0.183 - 20
R^2	0.9929	0.9918	0.9935	0.9930	0.9972	0.9973
Sensitivity (μ A/ μ M)	0.0809	0.0841	0.0536	0.0588	0.0214	0.0234
LoD (μ M)	-	0.150	-	0.087	-	0.169
LoQ (μ M)	-	0.501	-	0.290	-	0.563

References:

1. Cowman, S., G. Gethin, E. Clarke, Z. Moore, G. Craig, J. Jordan-O'Brien, N. McLain and H. Strapp (2012). "An international eDelphi study identifying the research and education priorities in wound management and tissue repair." J Clin Nurs **21**(3-4): 344-353.
2. Sharp, D. and J. Davis (2008). "Integrated urate sensors for detecting wound infection." Electrochemistry Communications **10**(5): 709-713.
3. Sharp, D., S. Forsythe and J. Davis (2008). "Carbon Fibre Composites: Integrated Electrochemical Sensors for Wound Management." Journal of Biochemistry **144**(1): 87-93.
4. Sharp, D. (2013). "Printed composite electrodes for in-situ wound pH monitoring." Biosensors and Bioelectronics **50**(0): 399-405.
5. McLister, A., J. Phair, J. Cundell and J. Davis (2014). "Electrochemical approaches to the development of smart bandages: A mini-review." Electrochemistry Communications **40**: 96-99.
6. Mehmood, N., A. Hariz, R. Fitridge and N. H. Voelcker (2014). "Applications of modern sensors and wireless technology in effective wound management." Journal of Biomedical Materials Research Part B-Applied Biomaterials **102**(4): 885-895.
7. Phair, J., M. Joshi, J. Benson, D. McDonald and J. Davis (2014). "Laser patterned carbon-polyethylene mesh electrodes for wound diagnostics." Materials Chemistry and Physics **143**(3): 991-995.
8. Bellin, D. L., H. Sakhtah, J. K. Rosenstein, P. M. Levine, J. Thimot, K. Emmett, L. E. Dietrich and K. L. Shepard (2014). "Integrated circuit-based electrochemical sensor for spatially resolved detection of redox-active metabolites in biofilms." Nat Commun **5**: 3256.
9. Webster, T. A., H. J. Sismaet, J. L. Conte, I. p. J. Chan and E. D. Goluch (2014). "Electrochemical detection of *Pseudomonas aeruginosa* in human fluid samples via pyocyanin." Biosensors and Bioelectronics **60**(0): 265-270.
10. Sismaet, H. J., Banerjee, B. McNish, S., Yongwook, C., Torralba, M., Lucas, S., Chan, A., Shanmugam, V.K., Goluch, E.D. "Electrochemical detection of *Pseudomonas* in wound exudate samples from patients with chronic wounds". Wound Repair and Regeneration **24**(366-372).
11. Sharp, D., P. Gladstone, R. B. Smith, S. Forsythe and J. Davis (2010). "Approaching intelligent infection diagnostics: Carbon fibre sensor for electrochemical pyocyanin detection." Bioelectrochemistry **77**(2): 114-119.
12. Wilson, R., Sykes, D.A., Watson, D, Rutman, A., Taylor, G.W., Cole, P.J. (1988) "Measurement of *Pseudomonas aeruginosa* phenazine in sputum and assessment of their contribution to sputum sol toxicity for respiratory epithelium", Infect. Immun. **56**: 2515–2517.
13. Hall, S., McDermott, C., Anoopkumar-Dukie, S., McFarland, A.J., Forbes, A., Perkins, A.V., Davey, A.K., Chess-Williams, R, Kiefel, M.J., Arora, D., Grant, G.D. (2016). Cellular Effects of Pyocyanin, a Secreted Virulence Factor of *Pseudomonas aeruginosa*. Toxins. **8**(8): 236

14. Muller, M. "Premature cellular senescence induced by pyocyanin, a redox-active *Pseudomonas aeruginosa* toxin" (2006). Free Radic Biol Med. **41**: 1670-1677
15. Muller, M. "Pyocyanin induces oxidative stress in human endothelial cells and modulates the glutathione redox cycle." (2002) Free Radic Biol Med. **33**:1527-33.
16. Bond, A. M. and B. S. Grabaric (1979). "Correction for background current in differential pulse, alternating current, and related polarographic techniques in the determination of low concentrations with computerized instrumentation." Analytical Chemistry **51**(3): 337-341.
17. Slowey, A. J. and M. Marvin-Dipasquale (2012). "How to overcome inter-electrode variability and instability to quantify dissolved oxygen, Fe(II), Mn(II), and S(-II) in undisturbed soils and sediments using voltammetry." Geochem Trans **13**(1): 6.
18. Górski, Ł., F. Ciepela and M. Jakubowska (2014). "Automatic baseline correction in voltammetry." Electrochimica Acta **136**(0): 195-203.
19. Nascimento, D. S., M. Insausti, B. S. F. Band and S. G. Lemos (2014). "Simultaneous determination of Cu, Pb, Cd, Ni, Co and Zn in bioethanol fuel by adsorptive stripping voltammetry and multivariate linear regression." Fuel **137**(0): 172-178.
20. Webster, T.A. and Goluch, E.D (2012). "Electrochemical detection of pyocyanin in nanochannels with integrated palladium hydride reference electrodes" Lab on a Chip **12**: 5195-5201

Figures:

Figure 1

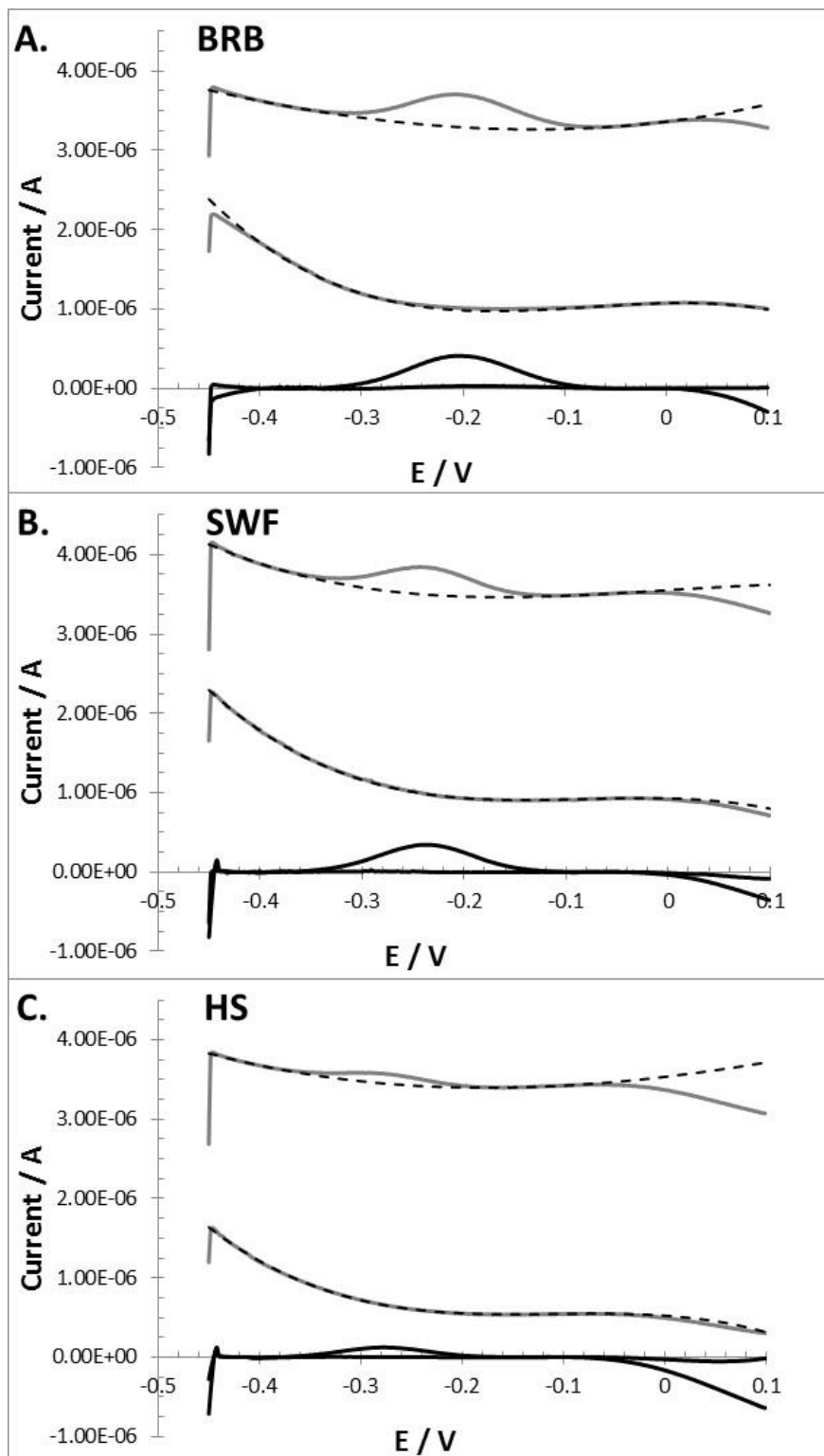


Figure 2

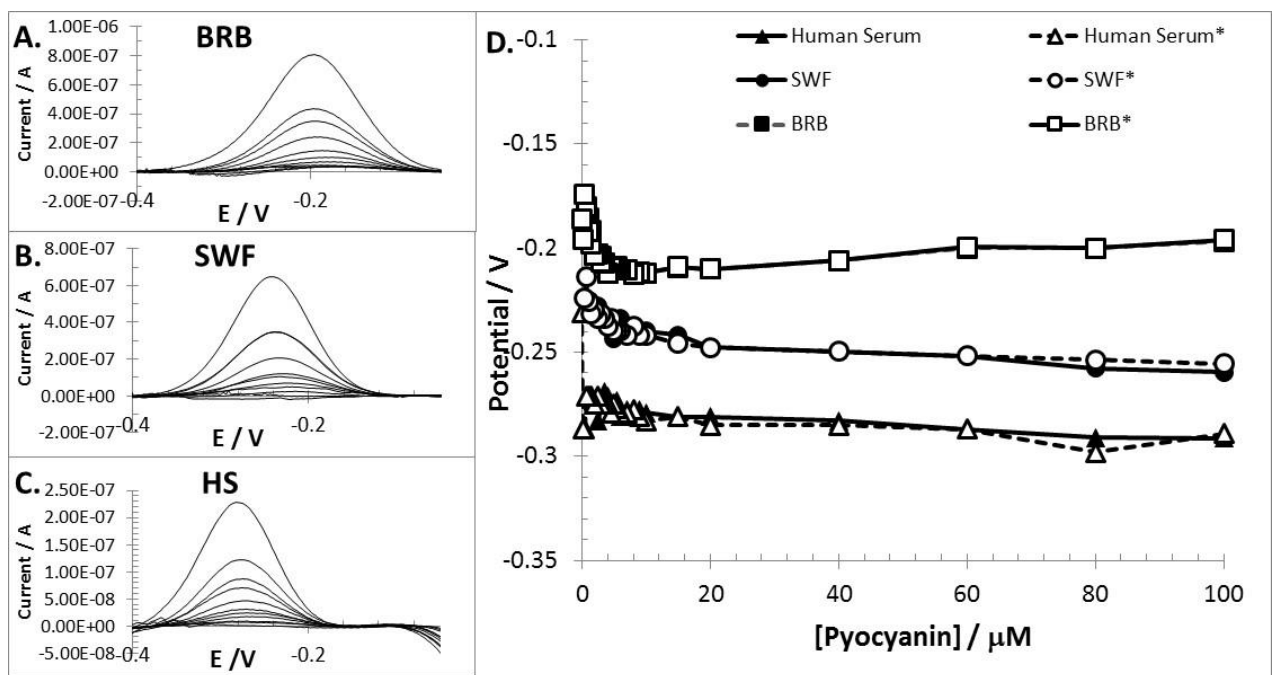


Figure 3

